REPORT DOCUMENTATION PAGE

Form Approved
OMB No. 0704-0188

1. REPORT DATE *(DD-MM-YYYY)*	2. REPORT TYPE	3. DATES COVERED *(From - To)*
Nov 1993	Technical Paper	

4. TITLE AND SUBTITLE

(See attached)

5a. CONTRACT NUMBER
F29601-92-C-0119

5b. GRANT NUMBER

5c. PROGRAM ELEMENT NUMBER

6. AUTHOR(S)

(See attached)

5d. PROJECT NUMBER
5730

5e. TASK NUMBER
00N2

5f. WORK UNIT NUMBER

7. PERFORMING ORGANIZATION NAME(S) AND ADDRESS(ES) AND ADDRESS(ES)

(See attached)

8. PERFORMING ORGANIZATION REPORT NUMBER

CPIA Publication 602, Vol II, Nov 93

9. SPONSORING / MONITORING AGENCY NAME(S) AND ADDRESS(ES)

Air Force Research Laboratory (AFMC)
AFRL/PRS
5 Pollux Drive
Edwards AFB CA 93524-7048

10. SPONSOR/MONITOR'S ACRONYM(S)

11. SPONSOR/MONITOR'S REPORT NUMBER(S)
PL-TP-94-30[illegible]

12. DISTRIBUTION / AVAILABILITY STATEMENT

(See attached)

13. SUPPLEMENTARY NOTES
These are technical papers, presentations that have been presented by AFRL/PRS from 1994.
1993 Propulsion Meeting, 15-19 Nov 93, Monterey, CA

14. ABSTRACT (maximum 200 words)

(See attached)

DISTRIBUTION STATEMENT A
Approved for Public Release
Distribution Unlimited

20040209 175

15. SUBJECT TERMS

16. SECURITY CLASSIFICATION OF:			17. LIMITATION OF ABSTRACT	18. NUMBER OF PAGES	19a. NAME OF RESPONSIBLE PERSON
a. REPORT	b. ABSTRACT	c. THIS PAGE			Kenette Gfeller or Leilani Richardson
Unclassified	Unclassified	Unclassified	SAR		19b. TELEPHONE NUMBER *(include area code)* DSN 525-5015 or 525-5016

MATERIALS CHARACTERIZATION AND DESIGN FOR SOLAR-THERMAL PROPULSION

M.J. DelaRosa and R.H. Tuffias
Ultramet
Pacoima, California

ABSTRACT

Solar-thermal propulsion relies on the conversion of concentrated solar energy into kinetic energy (in the exhaust gases) in order to provide thrust. Solar radiation is focused into a blackbody cavity in which the heat is absorbed and transferred to the hydrogen fuel through a thermal absorber/heat exchanger. Performance increases are obtained by increasing the efficiency of the absorber, thereby increasing the heat transfer to the hydrogen fuel. The absorber/exchanger itself provides structural properties, which involves the severe structural constraint of needing to withstand the high internal hydrogen pressure. Thus, the absorber/exchanger becomes the critical component in the thruster, and the enabling technology for the development of a successful solar-heated hydrogen propulsion system is a combination of materials and processing. The maximum operating temperature of a solar-thermal propulsion device is governed primarily by the strength and resistance to hydrogen degradation of the constituent materials at the operating temperature of 3000 K and above. Six candidate refractory materials were selected for investigation with regard to their potential for use in solar-thermal propulsion, with the aim of developing a properties and processing database in advance of designing, fabricating, and testing a solar-powered rocket engine (SPRE).

INTRODUCTION

The specific impulse of a rocket engine, a measure of performance, is proportional to the exhaust velocity of the propellant. For solar-thermal propulsion, in which the velocity of the propellant (hot hydrogen) is thermally derived through the conversion of concentrated solar energy into kinetic energy in the exhaust gases to provide thrust, achieving a high specific impulse requires maximizing the final propellant temperature and minimizing the molecular mass of the exhaust species. Hence, achieving a high specific impulse requires the use of very hot hydrogen. In a solar-thermal propulsion device, solar radiation is focused into a blackbody cavity in which the heat is absorbed and transferred to the hydrogen fuel through a thermal absorber/heat exchanger. Ultramet's version of this concept for a solar-powered rocket engine (SPRE) is illustrated schematically in Figure 1.

The enabling technology for the development of a successful solar-heated hydrogen propulsion system is a combination of materials and processing. Components such as thermal absorbers, heat exchangers, and nozzles must be fabricated from materials that can operate effectively at 3000 K and above while maintaining their structural integrity without degradation in the hot hydrogen environment.

This work focused on developing a materials, properties, and processing database for solar-thermal propulsion. Using the above criteria, five materials were selected for investigation: rhenium, hafnium carbide (HfC), tantalum carbide (TaC), niobium carbide (NbC), and zirconium carbide (ZrC). The physical properties of these materials are listed in Table I. The carbides were chosen due to their high melting points, while rhenium was chosen due to its excellent strength at high temperature. Tungsten was not considered because of its brittle nature and consequent difficulty in handling at room temperature, although it does not react with hydrogen and may meet the strength requirements for SPRE component use.

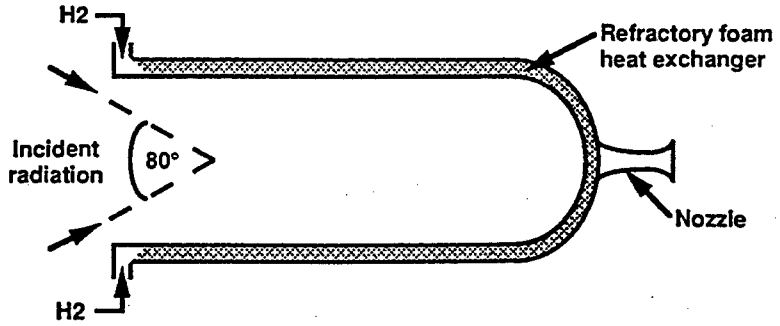

Figure 1. Schematic of preliminary SPRE design

Approved for public release; distribution unlimited.

This work was performed under contract F29601-92-C-0119 for the U.S. Air Force, Phillips Laboratory (Edwards AFB, CA), funded through the Air Force Small Business Innovation Research (SBIR) program.

Table I. Physical Properties of Carbon, Rhenium, and Refractory Carbides

	C	Re	HfC	TaC	NbC	ZrC
Molecular weight (g/mol)	12.01	186.21	190.54	192.96	104.92	103.23
Density (g/cm^3)	2.25	21.0	12.70	14.50	7.79	6.59
Melting point (°C)	--	3180	3890	3880	3500	3540
Boiling point (°C)	3550	5596	5400	5500	n/a	5100
Thermal conductivity (W/m·K)	150	71.2	22	22	30	20
Thermal expansion (ppm/K)	10.0	6.7	6.8	6.6	6.9	7.3
Specific heat (J/g·K)	0.84	0.138	0.20	0.19	0.35	0.37
Enthalpy (kJ/g, $H°_{Tm}$)	8.58	n/a	1.11	1.11	1.86	1.79
Hardness (kg/mm^2)	20	170	2300	2500	2400	2700
Crystal structure	hex	cph	fcc	fcc	fcc	fcc

[hex = hexagonal; fcc = face-centered cubic; cph = close-packed hexagonal]

The available fabrication processes for structural materials whose melting points exceed 3000°C are very limited: powder metallurgy, fiber-reinforced composite methods, and chemical vapor deposition (CVD). At present, powder metallurgy processes are not advanced enough to produce ceramic components with sufficient reliability, repeatability, and size. Composite technology is also not yet sufficiently advanced, especially in the area of high temperature fibers, other than carbon/carbon. Although refractory carbide-coated carbon/carbon composites have shown some promise in hot hydrogen, repeated high temperature cycling would likely cause substantial degradation in the protective coating, resulting in composite failure. In this work, Ultramet focused on developing a material properties database for the six materials selected and fabricated using CVD processing.

CHEMICAL VAPOR DEPOSITION

The CVD process proceeds by a series of mechanistic steps. In its simplest form, these include transport of the reactants to the surface, adsorption of the reactants on the surface, chemical reaction, desorption of the gaseous reaction products, and transport of the products away from the surface. The fact that both the reactants and products are transported in the vapor phase makes the process amenable to fabricating or coating complex shapes, infiltrating porous bodies, and coating powders uniformly.

The advantages of CVD processing include the following:

- versatility: virtually every element and ceramic compound can be formed by CVD
- low processing temperature: typically 25-50% of the melting temperature
- non-line-of-sight process
- ability to deposit to net shape/conformal to substrate surface
- high purity (typically 99.99%+)
- high density (nearly 100% of theoretical)
- high rate of formation (typically 100-500 μm/hr)

Rhenium is formed by the thermal decomposition of rhenium pentachloride, according to the following reaction:

$$ReCl_5 \longrightarrow Re + 5/2Cl_2$$

Metal carbides are typically formed by reacting a halide of the metal with a carbon source such as methane, as in the following reactions for HfC, TaC, NbC, and ZrC respectively:

$$HfCl_4 + CH_4 \longrightarrow HfC + 4HCl$$
$$TaCl_5 + CH_4 \longrightarrow TaC + 4HCl + 1/2Cl_2$$
$$NbCl_5 + CH_4 \longrightarrow NbC + 4HCl + 1/2Cl_2$$
$$ZrCl_4 + CH_4 \longrightarrow ZrC + 4HCl$$

COMPONENT FABRICATION

CVD fabrication of SPRE components involved three material configurations:

1. thermal absorber/heat exchanger: porous open-cell foam
2. skin for foam absorber/exchanger: solid coating
3. nozzle: solid free-standing shape (shell)

Free-standing shapes or shells are fabricated by CVD by forming the desired material on a mandrel that replicates the desired shape, and then removing the mandrel by chemical or other means.

Porous foams are fabricated by CVD by infiltrating a carbon foam skeleton, which has first been machined to the desired geometry, with the desired material. Infiltration requires that the CVD reaction take place within the porous structure, which is accomplished by standard gas transport techniques involving pressure and/or thermal gradients. The foam can then be "skinned" with a solid exterior coating by CVD or other means.

CHARACTERIZATION

Foam samples were fabricated and characterized according to the materials/testing matrix shown in Table II:

- Mechanical: flexural strength, flexural modulus, compressive strength
- Thermal: thermal expansion coefficient (CTE), specific heat, thermal diffusivity, thermal conductivity
- Hot hydrogen stability: 3000 K for three 10-minute cycles
- High temperature creep: 3000 K under 50-psi load

Table II. Materials/Testing Matrix

	Re	HfC	TaC	NbC	ZrC*
Flexural strength measurement	X	X	X		
Flexural modulus measurement	X	X	X		
Compressive strength measurement	X	X	X		
CTE evaluation	X			X	
Specific heat measurement	X	X	X		
Thermal diffusivity measurement	X	X	X		
Thermal conductivity measurement	X	X	X		
3000 K H_2 testing				X	
3000 K creep testing				X	

* Samples currently being fabricated and evaluated

MECHANICAL PROPERTIES

Rhenium, hafnium carbide, and tantalum carbide foams were tested for room temperature flexural strength and flexural modulus, as well as compressive strength up to 2750°C. The room temperature flexural strength and modulus of 65-ppi (pores-per-inch) rhenium, HfC, and TaC foams are shown in Figures 2 and 3, respectively. The compressive strength of 65-ppi rhenium, HfC, and TaC foams over the range 20-2750°C is shown in Figure 4. The compressive strength value for HfC foam at 1.14 g/cm^3 bulk density is anomalously low, which may be caused by nonuniform infiltration of the sample. Mechanical properties measurements for NbC foam remain to be performed.

THERMAL EXPANSION

The thermal expansion coefficient is an important factor in the design and high temperature performance of the SPRE. Rhenium foam samples, 0.25 x 0.50 x 1.0", were fabricated to densities of 1.2, 1.5, and 1.8 g/cm^3, and CTE was measured from room temperature to 1600°C (see Figure 5). There is a variation in the CTE of the rhenium foams at lower densities in the lower temperature regions. This is thought to be caused by a contribution from the carbon foam substrate, perhaps due to carbon diffusion into the rhenium coating. At higher densities, the contribution of this thin diffusion layer is small compared to that of the thicker pure rhenium.

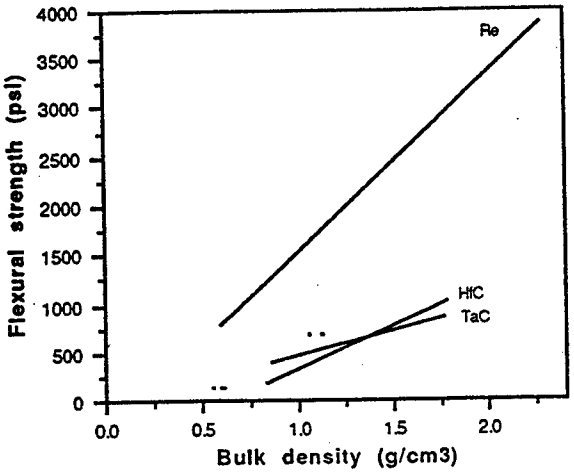

Figure 2. Room temperature flexural strength vs. bulk density for rhenium, HfC, and TaC foam

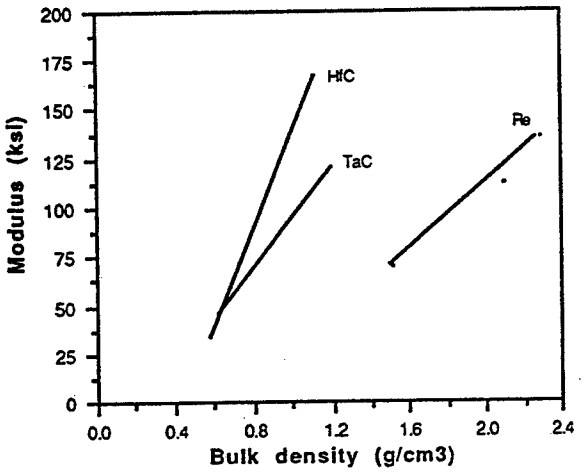

Figure 3. Room temperature flexural modulus vs. bulk density for rhenium, HfC, and TaC foam

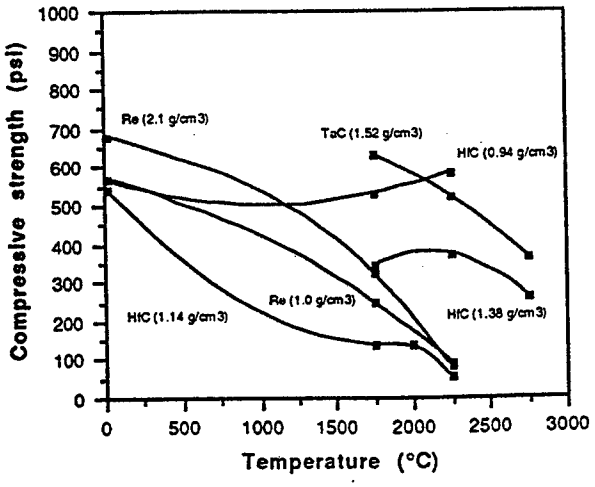

Figure 4. Compressive strength vs. bulk density and temperature for rhenium, HfC, and TaC foam

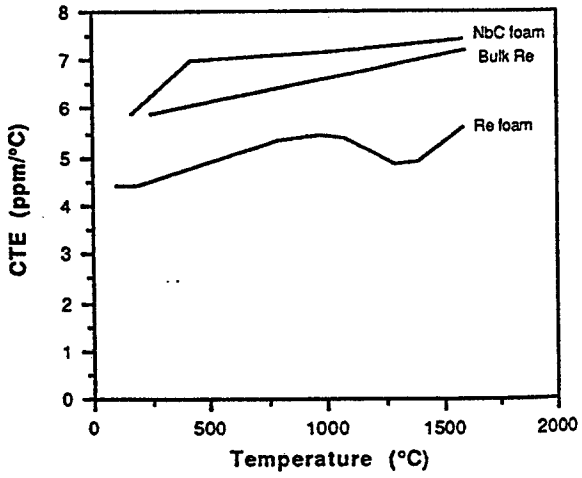

Figure 5. CTE vs. temperature for bulk CVD rhenium, rhenium foam, and NbC foam

For CTE measurement of bulk CVD rhenium, a rhenium tube was fabricated having dimensions of 0.25" O.D. x 0.21" I.D. x 1.0" long. A CTE mismatch was found to exist between the bulk rhenium and the rhenium foam (see Figure 5). The higher CTE of the bulk rhenium would result in some compression of the rhenium foam heat exchanger caused by the greater expansion of the inner solid rhenium absorber. CTE measurements for HfC and TaC foam remain to be performed.

The CTE of NbC foam was also measured between room temperature and 1600°C. Some hysteresis was initially observed, attributed to a mixture of NbC and Nb_2C in the composition. During subsequent CTE measurements, the degree of hysteresis decreased due to partial conversion of the Nb_2C to NbC. To confirm this hypothesis, the sample was heat treated in argon at 2000°C for 30 minutes, and the CTE measured again. The hysteresis disappeared, and the measured CTE was 7.38 ppm/°C (see Figure 5), in excellent agreement with the reported literature value of 7.31 ppm/°C.

THERMAL PROPERTIES

A critical part of the SPRE design is the heat exchanger and the amount of thermal energy it can transmit to the working fluid. Samples of rhenium, hafnium carbide, and tantalum carbide foam were measured for specific heat using the Bunsen ice calorimeter technique. The results are shown in Figures 6-8. The thermal diffusivity of these foams was then measured by laser flash diffusivity. In order to average the energy of the laser flash across the foam pores and ligament ends, graphite paste was applied to one face of the 0.75" diameter x 0.375" thick foam disks. After the thermal diffusivity was measured, the known contribution from the graphite layer was subtracted, thereby giving the contribution solely from the foam. Thermal diffusivity is shown as a function of temperature in Figures 9-11.

Thermal conductivity (λ), shown as a function of temperature in Figures 12-14, was then determined by combining the thermal diffusivity (α), density (ρ), and specific heat (C_p) of these materials, as follows:

$$\lambda = \alpha \rho C_p$$

Thermal properties measurements for NbC foam remain to be performed.

EROSION IN HOT HYDROGEN

Five samples of NbC foam were exposed to 3000 K hydrogen for one to three 10-minute cycles. A weight loss of ≈4% was observed after the first cycle, with negligible change thereafter. The degree of weight loss corresponds roughly to the weight fraction of carbon associated with each of the samples (the underlying carbon foam skeleton). The weight loss is therefore associated with etching of the carbon by hydrogen. Scanning electron microscopy of the samples verified this assumption by showing the carbon core to be absent in samples that had been exposed to hot hydrogen, as shown in Figure 15. The NbC coating remained intact in all cases. Table III shows the hot hydrogen test data.

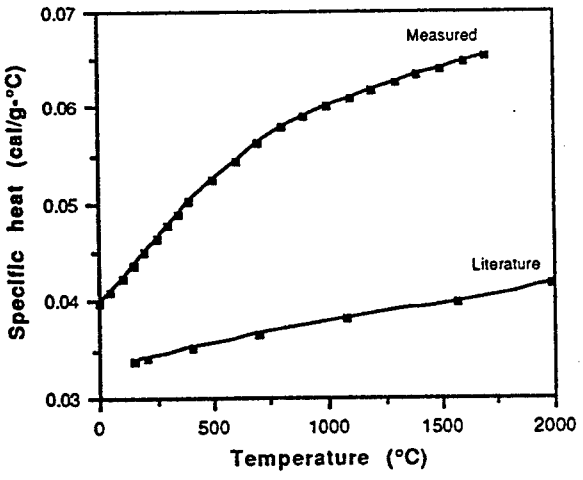

Figure 6. Specific heat vs. temperature for rhenium foam

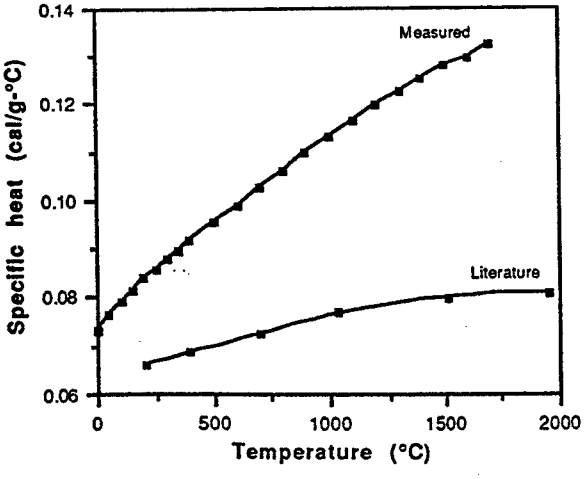

Figure 7. Specific heat vs. temperature for HfC foam

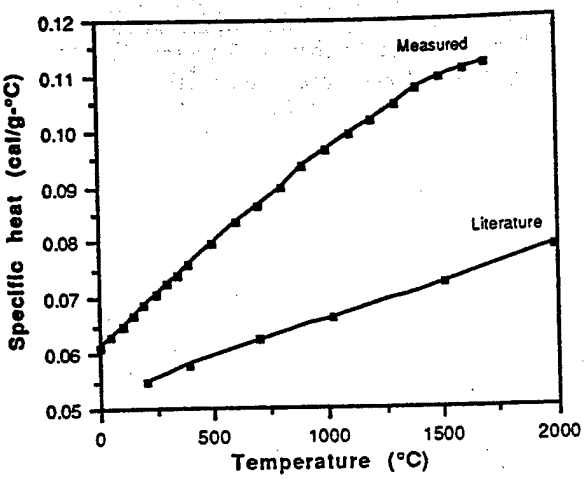

Figure 8. Specific heat vs. temperature for TaC foam

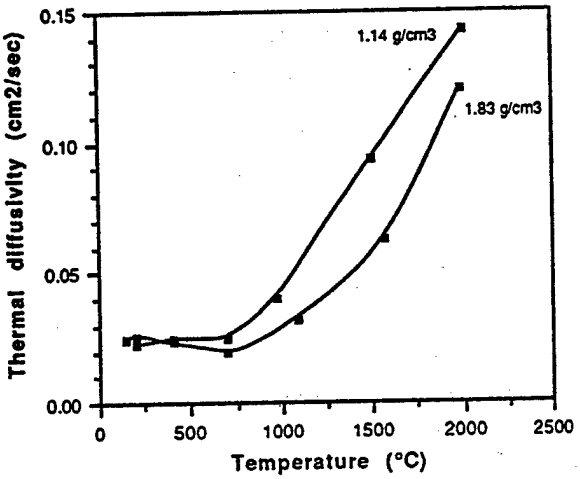

Figure 9. Thermal diffusivity vs. temperature for rhenium foam

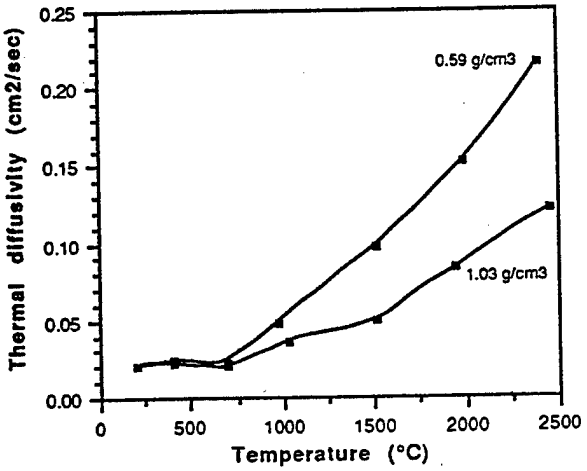

Figure 10. Thermal diffusivity vs. temperature for HfC foam

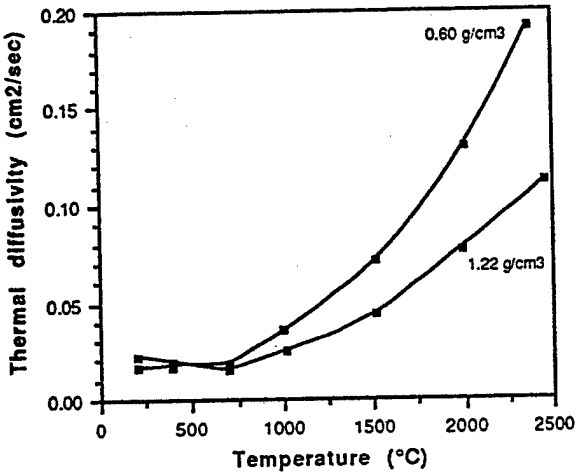

Figure 11. Thermal diffusivity vs. temperature for TaC foam

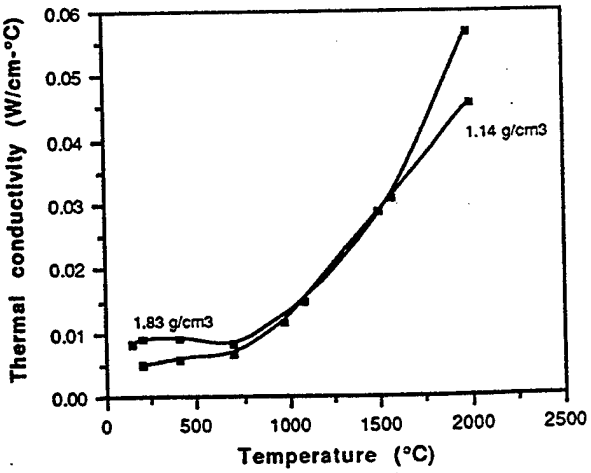

Figure 12. Thermal conductivity vs. temperature for rhenium foam

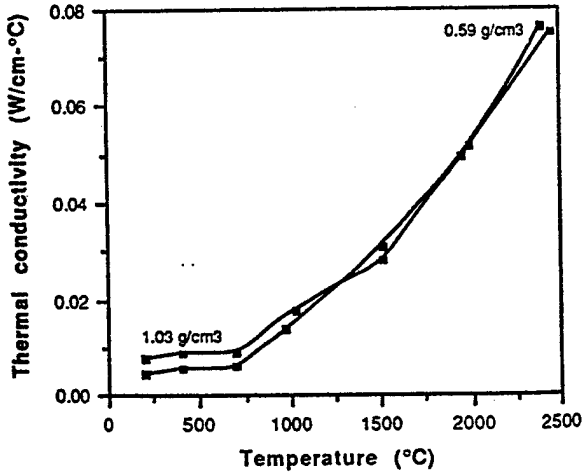

Figure 13. Thermal conductivity vs. temperature for HfC foam

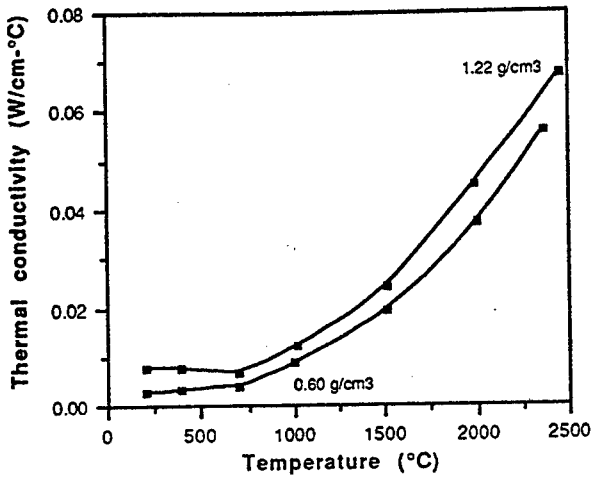

Figure 14. Thermal conductivity vs. temperature for TaC foam

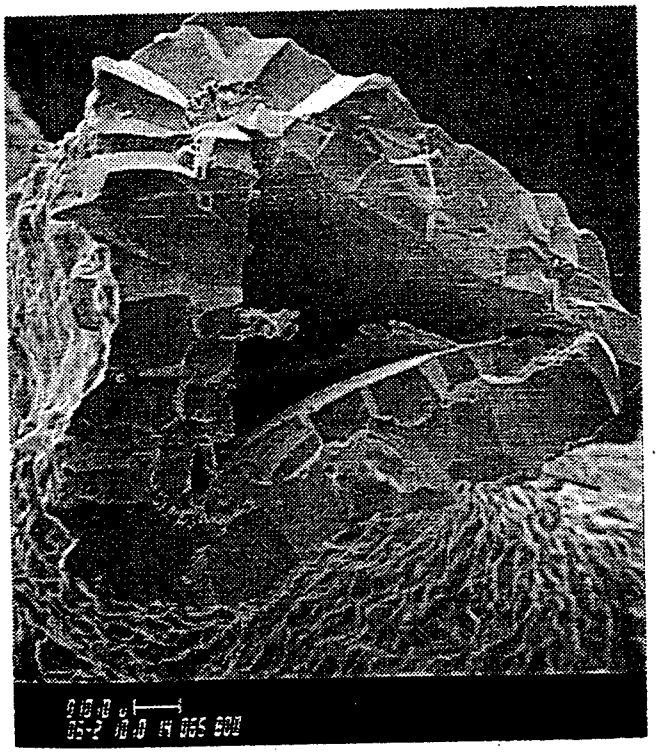

Figure 15. SEM micrograph of NbC foam following 3000 K hydrogen exposure

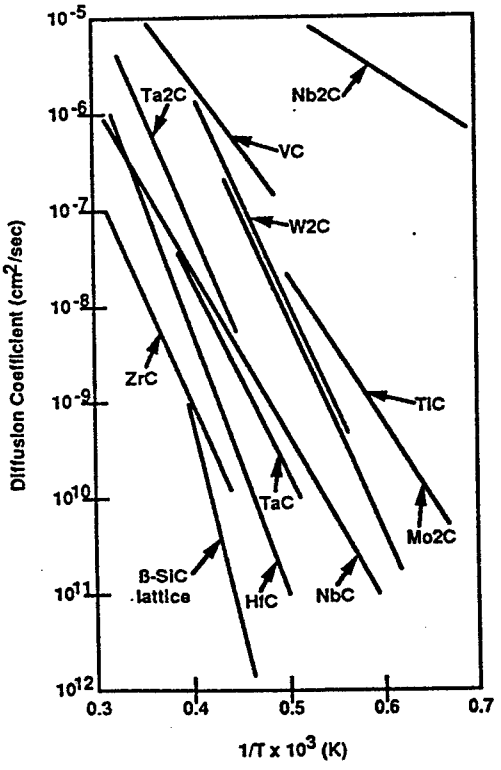

Figure 16. Diffusivity of carbon in refractory carbides

Table III. Hot Hydrogen Test Results

Sample # (3)	Initial weight (mg)	3000 K/H2/10-min cycle								3000 K/50 psi/10-min			
		#1		#2		#3		Total		Load direction			
		ΔWt (%)	ΔL (%)	ΔWt (%)	ΔL (%)	ΔWt (%)	ΔL (%)	ΔWt (%)	ΔL (%)	ΔL (%)	ΔH (%)	ΔWt (%)	#H2 cycles
#1-1 (ring)	20,170	-2.9	0	N/A	N/A	N/A	N/A	-2.9	0				
#1-2 (ring)	19,379	-2.8	0	-0.09	0	-0.08	0	-3.0	0				
#2-2 (bar) (1)	482	-6.2	-1.0	N/A	N/A	N/A	N/A	-6.2	-1.0	-0.9	0	0.5	1
#2-3 (bar) (2)	583	-4.3	--	0.09	--	N/A	N/A	-4.2	-1.4	-0.8	0	0.4	2
#2-4 (bar) (2)	479	-4.2	--	0.10	--	0.04	--	-4.0	-1.8	-0.2	0	0.3	3
#2-1 (bar) (2)	562	N/A	N/A	N/A	N/A	N/A	N/A	N/A	N/A	-2.0	0	-0.1	0

(1) thick black surface on O.D. prior to testing (probably excess carbon)
(2) 1% weight change ≈5 mg
(3) carbon skeleton weight ≈3-5%

At 3000 K, the diffusion of carbon through NbC (and other carbides as well, as shown in Figure 16) is quite rapid, with diffusivities ranging from 10^{-6} to 10^{-7} cm^2/sec. This imposes limits on the useful lifetime of carbide-coated graphite or carbon/carbon. For infiltrated foams, however, the loss of carbon is not critical since the mechanical properties of the material are due almost entirely to the coating rather than the carbon core.

HIGH TEMPERATURE CREEP

Three of the NbC foam samples that had previously undergone hot hydrogen testing, as well as a fresh sample, were exposed to 3000 K helium for 10 minutes while under a static load of 50 psi. The data in Table III again show minimal dimensional change associated with the test. Sample #2-1 is noteworthy in that it underwent negligible weight change, further supporting the assertion that the weight changes are associated with hydrogen etching of the carbon cores of the foam ligaments.

PROTOTYPE SPRE DESIGN

A prototype SPRE is currently being fabricated for verification of processing techniques and material properties. This design, shown in Figure 1, has a length-to-diameter ratio of approximately 10:1, creating, in essence, a blackbody. The design aims to trap and absorb as much incident solar radiation as possible, thereby maximizing the thermal energy to be transferred to the gaseous hydrogen propellant. This design is being modeled and refined in collaboration with AlliedSignal Aerospace (Torrance, CA).

CONCLUSIONS

The design and fabrication of a solar-powered rocket engine is being investigated using refractory foam as the heat exchanger and refractory metal for the thermal absorber and nozzle. Rhenium, hafnium carbide, tantalum carbide, and niobium carbide were investigated for use in the hot hydrogen environment. The room temperature flexural strength and modulus, high temperature compressive strength, thermal expansion, and thermal conductivity of these materials were measured. These tests will be repeated, however, as some of the data are inconsistent. Additional testing also remains to complete the test matrix, including evaluation of zirconium carbide foam. A prototype design is being explored for fabricability and performance.

ACKNOWLEDGEMENTS

This work was performed under contract F29601-92-C-0119 for the U.S. Air Force, Phillips Laboratory (Edwards AFB, CA), funded through the Air Force Small Business Innovation Research (SBIR) program. Ultramet would like to thank the Air Force project manager, Kristi K. Laug, for her input and support over the course of the program; Energy Materials Testing Laboratory (Biddeford, ME) for performing the high temperature compressive testing and laser flash diffusivity testing for determination of thermal conductivity; and Babcock & Wilcox (Lynchburg, VA) for performing the hot hydrogen and 3000 K creep testing.